Kent Academic Repository

Chapple, Simon A., Smith, Tanya M. and Skinner, Matthew M. (2024) *Testing the patterning cascade model of cusp development in Macaca fascicularis mandibular molars.* Archives of Oral Biology, 167 . ISSN 0003-9969.

Testing the patterning cascade model of cusp development in *Macaca fascicularis* mandibular molars

Simon A. Chapple [a,*], Tanya M. Smith [b], Matthew M. Skinner [c]

[a] *School of Anthropology and Conservation, University of Kent, Canterbury CT2 7NZ, United Kingdom*
[b] *Griffith Centre for Social and Cultural Research and Australian Research Centre for Human Evolution, Griffith University, Southport, Queensland 4222, Australia*
[c] *Max Planck Institute for Evolutionary Anthropology, Leipzig, Germany*

A R T I C L E   I N F O

A B S T R A C T

Objective: Molar crown configuration plays an important role in systematics, and functional and comparative morphology. In particular, the number of cusps on primate molars is often used to identify fossil species and infer their phylogenetic relationships. However, this variability deserves renewed consideration as a number of studies now highlight important developmental mechanisms that may be responsible for the presence of molar cusps in some mammalian taxa. Experimental studies of rodent molars suggest that cusps form under a morphodynamic, patterning cascade model of development (PCM) that involve the iterative formation of enamel knots. This model posits that the size, shape and location of the first-forming cusps determines the presence and positioning of later-forming cusps.
Design: Here we test whether variation in accessory cusp presence in 13 *Macaca fascicularis* mandibular second molars (M2s) is consistent with predictions of the PCM. Using micro-CT, we imaged these M2s and employed geometric morphometrics to examine whether shape variation in the enamel-dentine junction (EDJ) correlates with accessory cusp presence.
Results: We find that accessory cusp patterning in macaque M2s is broadly consistent with the PCM. Molars with accessory cusps were larger in size and possessed shorter relative cusp heights compared to molars without accessory cusps. Peripheral cusp formation was also associated with more centrally positioned primary cusps, as predicted by the PCM.
Conclusions: While these results demonstrate that a patterning cascade model is broadly appropriate for interpreting cusp variation in *Macaca fascicularis* molars, it does not explain all manifestations of accessory cusp expression in this sample.

1. Introduction

Much of what is known about mammalian tooth morphogenesis and the growth of multicuspid teeth comes from research in experimental genetics, evolutionary morphology, and embryology, and has led to the development of models through which variability in tooth crown morphology can be interpreted. In particular, studies of developing murine teeth (Jernvall, 2000; Jernvall & Thesleff, 2000; Salazar-Ciudad & Jernvall, 2002; Kassai et al., 2005), and computational modelling of mammalian tooth germs (Salazar-Ciudad & Jernvall, 2002, 2010), have shown that the mechanisms responsible for the patterning of multicuspid tooth crowns involve the punctuated and iterative appearance of embryonic signalling centres known as enamel knots. These enamel knots are thought to be equivalent to the signalling centres responsible for the epithelial appendage patterning of scales, feathers, limb buds and hair follicles (Niswander & Martin, 1992; Thesleff & Nieminen, 1996; Vaahtokari et al., 1996). In these examples, pattern formation is regulated and controlled by the spatial distribution of signalling centres at which there is interaction between differentially diffusing activatory and inhibitory morphogens.

Enamel knots have been implicated in the activation of cell proliferation and folding of the inner enamel epithelium, which determines the shape and size of the tooth (Jernvall & Thesleff, 2000; Kassai et al., 2005). They also produce proteins that inhibit the formation of new enamel knots nearby, creating a temporospatial zone of inhibition. As such, new signalling centres can only form outside the zones of
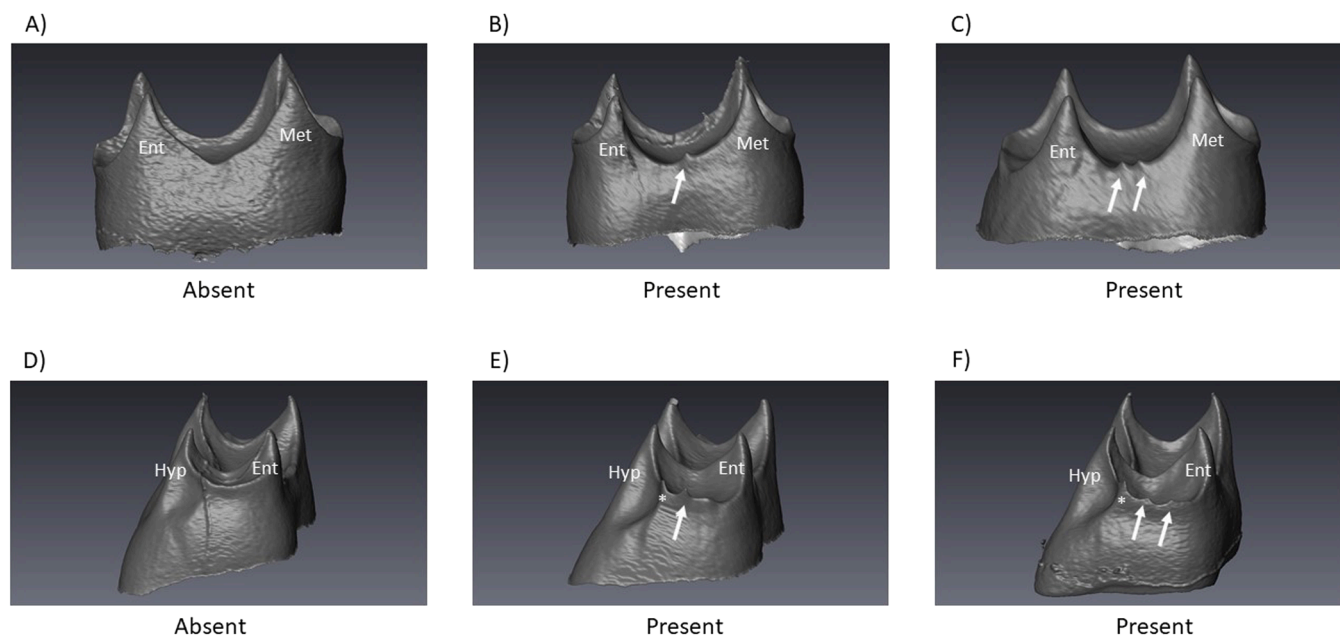
Fig. 1. Accessory Cusp Scoring as 'Absent' or 'Present'. Above - Lingual accessory cusp (LAC). Lingual view. (A) No evidence of a dentine horn; (B) Presence of one accessory cusp on the lingual ridge; (C) Presence of two distinct accessory cusps on the lingual ridge. Below - Distal accessory cusp (DAC). Distal view. (D) No evidence of a dentine horn; (E) Presence of one accessory cusp on the distal ridge; (F) Presence of two distinct accessory cusps on the distal ridge. Ent = Entoconid, Met = Metaconid, Hyp = Hypoconid. *denotes the presence of a distal hypoconid shoulder that is not included in the scoring procedure.

inhibition of previously formed enamel knots. The primary enamel knot appears in the tooth germ at the tip of the dentine horn of the first cusp and induces the appearance of secondary enamel knots (Jernvall & Thesleff, 2000). These secondary enamel knots appear along the inner enamel epithelium at the sites of future cusps. They influence the potential expression of further cusps through an interplay between the timing and spacing of enamel knot initiation, the overall size of the tooth germ, and the duration of crown growth before mineralisation. These interactions represent the foundation and principle of the patterning cascade model (PCM), which suggests that cusp formation is not predetermined but based on the interplay between these various processes and interactions (Salazar-Ciudad & Jernvall, 2002). Importantly these developmental parameters can be assessed in fully-formed teeth by studying the overall size of a tooth, the distance between neighbouring cusps, and the height of each cusp.

The patterning cascade model has successfully explained variation in cusp number and patterning among Lake Ladoga ringed seals (Jernvall, 2000). Among primates, the vast majority of work has been conducted with Hominidae molars, and findings are generally consistent with predictions made by the PCM. For example, Kondo and Townsend (2006) and Harris (2007) showed that an accessory cusp was more likely to be present on larger molars of humans, which the PCM would suggest was due to a reduced spatial constraint on secondary enamel knot formation within the tooth germ. Similarly, Skinner and Gunz (2010) report the presence of dentine horns on the distal margin of the enamel-dentine junction (EDJ) of chimpanzee mandibular molars that were consistent with PCM predictions. More recently, Ortiz et al. (2018) examined 17 living and fossil hominoid species and reported that while the majority of accessory cusp expression could be explained by the PCM, some accessory cusps pointed to potential deviations from this developmental model. Extensive research in other primate clades however, is currently lacking. Monson (2012) and Winchester (2016) noted some discordance between certain aspects of observed cercopithecine molar morphology and PCM-predicted morphology, but this has yet to be formally and extensively studied.

In this study, we examine *Macaca fascicularis* molars to assess whether the processes controlling accessory cusp expression are consistent with the predictions of the PCM. Papionini.

molars are ideal candidates for testing the predictions of the PCM because they variably express both distal and lingual accessory cusps, and have a simple primary cusp patterning that can be used to easily divide teeth into mesial, distal, lingual and buccal sections. In a sample of *Macaca fuscata* lower second molars, Swindler (2002) reports the presence of lingual accessory cusps in 38 % of specimens, and in 56.8 % of *Papio* first lower molars. Several authors also note the variable but observable presence of distal accessory cuspules in Papionini molars, which extend from the distal marginal ridge and often project backwards towards the succeeding tooth (Swindler, 1983, 2002; Szalay & Delson, 2013). More recent observations at the EDJ support these earlier reports regarding the variability of these features, and demonstrate that they are clearly visible and easily delineated using micro-CT technology (Chapple & Skinner, 2023a). As accessory cusps in Papionini molars are variable, plainly and clearly observable, and are easily delineated features, they are an ideal candidate for testing the predictions of the PCM. By limiting our sample to lower second molars from a single population of *Macaca fascicularis*, we remove several sources of variation that are known to influence crown morphology, such as phylogeny and tooth position, to provide the first comprehensive assessment of the PCM in Cercopithecine molars.

We analyse the correlation between EDJ shape (including overall EDJ size, dentine horn height, and dentine horn spacing) and the variable presence of lingual accessory cusps (LAC) and distal accessory cusps (DAC) in macaque mandibular second molars (M2s). While accessory cusps in these positions are often referred to as cusp 7 and cusp 6 respectively, we follow Davies et al. (2021) in using more generalized terms as they are inherently free of homologous interpretation and allow for the presence of multiple cusps along their respective ridge. Based on the predictions of the PCM, a LAC or DAC is less likely to form when tooth size is comparatively small, and when the primary dentine horns are large or closely spaced. Conversely, a LAC or DAC cusp is more likely to form with increased tooth size, and relatively small and/or widely spaced cusps.
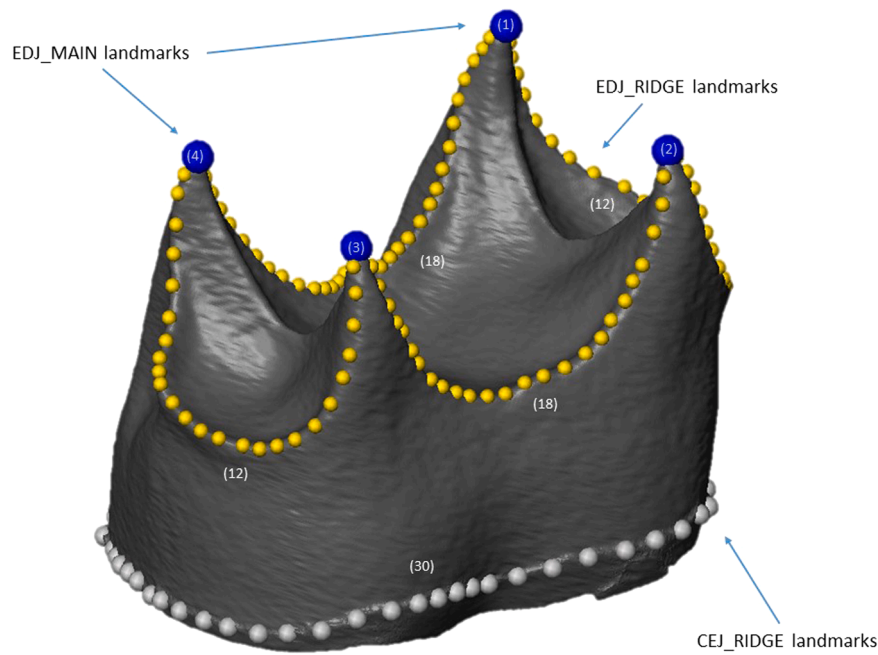
Fig. 2. Disto-lingual view of a digital model of a macaque lower second molar crown with the enamel cap removed to reveal the surface of the EDJ. Landmarks used to capture the size and positioning of the primary cusps and tooth outline are shown as spheres. Blue spheres are EDJ_MAIN landmarks, yellow spheres are EDJ_RIDGE curve landmarks, and the grey spheres are the CEJ_RIDGE curve landmarks.

2. Materials and Methods

2.1. Study sample

To test the relationship between EDJ shape and accessory cusp presence it is best to limit taxonomic and metameric variation. The study sample was thus restricted to M2s of *Macaca fascicularis* (n = 13) from the Wake Forest University Primate Centre (Winston-Salem, NC). The majority of individuals from this facility were captive, and those with signs of dental or skeletal pathology were excluded. Specimens were chosen to have relatively equal numbers of those with and those without LAC or DAC cusps, while also restricting the sample to those individuals with relatively unworn or undamaged mandibular second molars. As *Macaca fascicularis* molars become worn early in life, acquiring unworn, undamaged molars was a challenge that resulted in a comparatively small sample size.

3. Scoring Procedure

Accessory cusp scoring was restricted to dichotomous 'Absent' and 'Present' categories to maximise the sample size of each group. As such, the 'Present' category encompasses various manifestations of LAC and DAC expression, including the occurrence of multiple dentine horns along the corresponding ridge (Fig. 1). The LAC was scored as present if one or more dentine horns were observed between the metaconid and entoconid cusps. The DAC was scored as present if one or more dentine horns were observed between the entoconid and hypoconid cusps. Importantly, while there is reason to question whether the distal extension and shouldering of the hypoconid in some specimens is a true dentine horn (in that it was initiated and formed by a secondary enamel knot), it was not present in any of the specimens within the 'Absent' category (see Davies et al., 2021 for further discussion of the relationship between 'shouldering' and accessory cusp presence).

4. Micro-CT, image filtering and tissue segmentation

Dentitions were scanned with one of two micro-CT scanners (Harvard University Centre for Nanoscale Systems X-Tek HMXST 225 CT;

Nikon Corporation X-Tek XT H225 CT) with voxel sizes between 17 and 28 cubic microns. Scanning was conducted under standard operating conditions (current, energy, and metallic filters) following established protocols (Olejniczak et al., 2007; Feeney et al., 2010; Smith et al., 2012; Kato et al., 2014). Image stacks for each molar were then filtered to facilitate tissue segmentation using a 3D mean-of-least-variance filter with a kernel size of one. This filtering process sharpens the boundaries between enamel and dentine (Schulze & Pearce, 1994), allowing for a clearer segmentation of tissue types, while having minimal effect on the accurate reconstruction of the EDJ surface (Skinner et al., 2008). Filtering was implemented using MIA open source software (Wollny et al., 2013).

Filtered image stacks were segmented in Avizo 6.3 using a semi-automatic process that separates voxels based on greyscale values. After segmentation, the EDJ was reconstructed as a triangle-based surface model. As a final step before landmark collection, accessory cusps were cropped from EDJ surface models with Geomagic Studio 2014 (3D systems, Rock Hill) in order to quantify the shape of the marginal ridge (Supplementary Figure 1). This process allowed for the complete placement of landmarks around the marginal ridge of the tooth without the influence of potentially confounding dentine horn-like features.

5. Landmark collection and derivation of homologous landmark sets

EDJ surface models were used to create three sets of 3D landmarks in Avizo 6.3. The first set (EDJ_MAIN) were placed at the tips of the dentine horn for each primary cusp (Fig. 2). The second set (EDJ_RIDGE) were placed along the marginal ridge that connects the four dentine horns, creating a continuous set of landmarks around the basin of the tooth. The third set of landmarks (CEJ_RIDGE) were placed along the cementum-enamel junction. In cases where sections of the CEJ were missing due to cervical enamel fracture, the location of these landmarks were estimated. In two specimens, the CEJ could not be reliably estimated and thus were not including in any analyses incorporating this landmark set.

Geometrically homologous semi-landmarks (Gunz et al., 2005) for the EDJ_RIDGE and CEJ_RIDGE were then derived in R using the
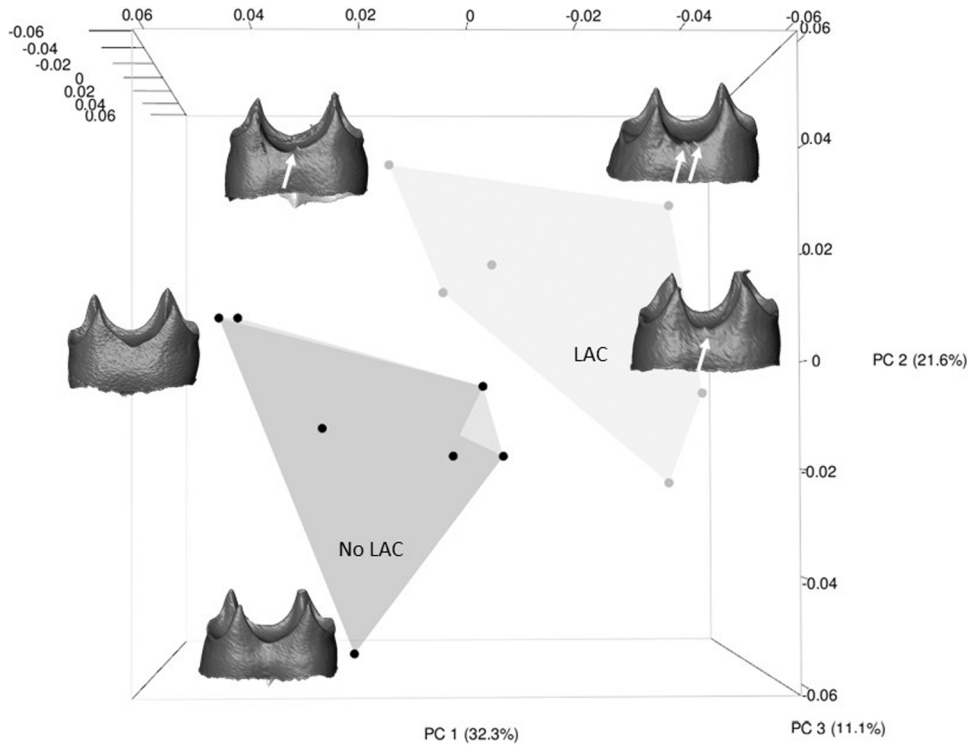
Fig. 3. 3D plot of the first three principal components of an analysis of EDJ ridge shape variation between specimens with variable expression of a LAC. Accessory cusp absence corresponds to the lighter grey convex hull and grey spheres. Accessory cusp presence corresponds to the darker grey convex hull and black spheres. 3D plots of the whole tooth analysis and isolated lingual ridge are provided in the supplementary materials.

packages Morpho (Schlager et al., 2017) and princurve (Cannoodt & Bengtsson, 2019).

This process involves the fitting of a smooth curve through the landmarks of the EDJ and CEJ ridge using a cubic-spline function. A fixed number of equally spaced semilandmarks were then placed along the curve; the EDJ_RIDGE had 18 landmarks along the buccal and lingual ridges, and 12 along the mesial and distal ridges. The CEJ_RIDGE had a single set of 30 landmarks that surrounded the CEJ. While the EDJ_MAIN landmarks remain fixed, these landmarks attributed to the EDJ_RIDGE and CEJ_RIDGE are treated as semi-landmarks and allowed

Fig. 4. (A) Plot of the first and second principal components of an analysis of whole tooth shape variation between molars with variable expression of a LAC. (B) Centroid size of macaque lower second molars with and without a LAC. (C) Exaggerated wireframe model of the shape change along PC1 (exaggerations defined as two standard deviations from the mean). Lingual view. (D) Exaggerated wireframe model of the shape change along PC2. Lingual view.
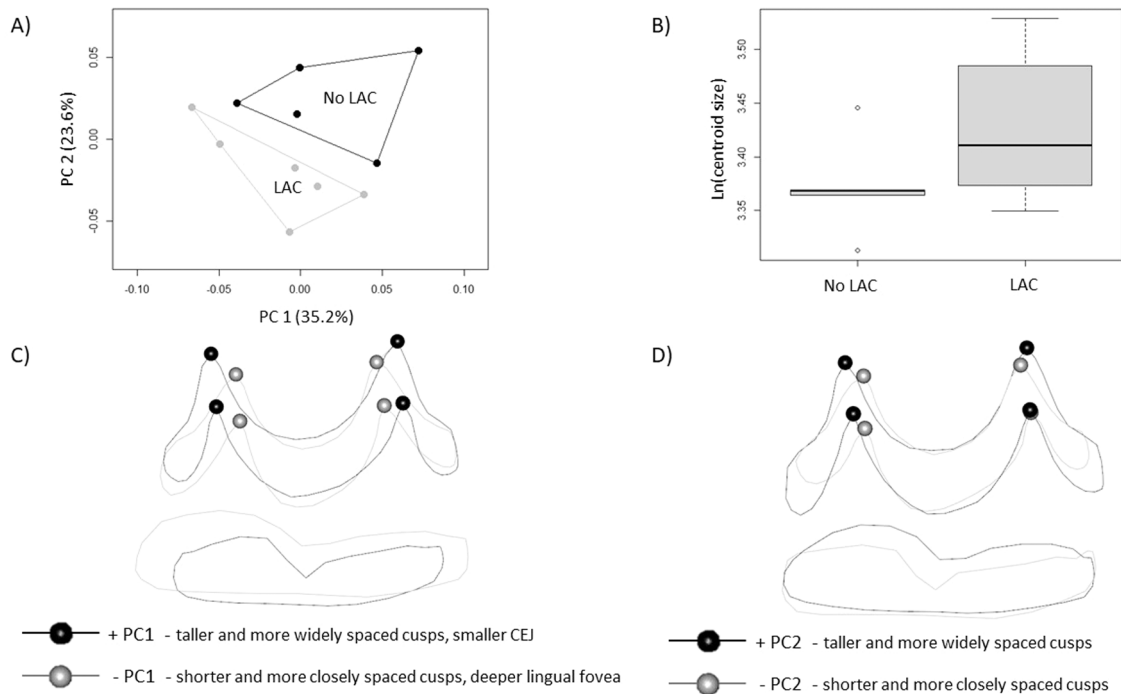
Fig. 5. Plot of the first and second principal components of an analysis of EDJ ridge shape variation between molars with variable expression of a LAC. (B) Centroid size of macaque lower second molars with and without a LAC. (C) Exaggerated wireframe model of the shape change along PC1 (exaggerations defined as two standard deviations from the mean.) Lingual view. (D) Exaggerated wireframe model of the shape change along PC2. Lingual view.
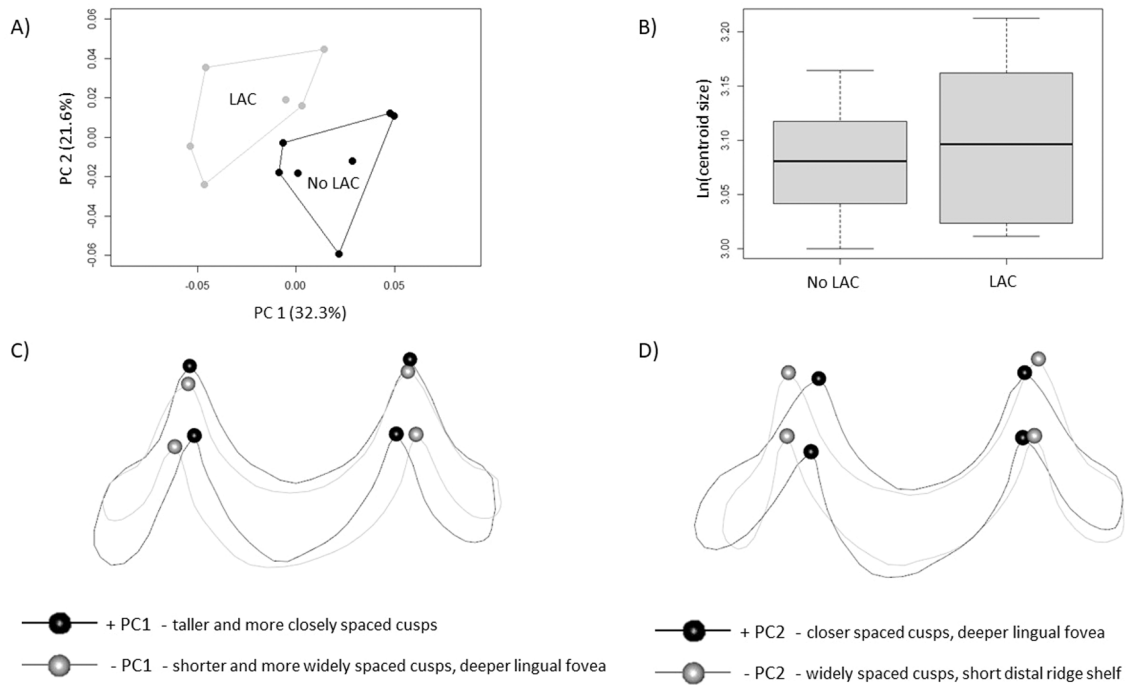
to slide along their respective curves to minimise the bending energy of the thin-plate spline interpolation function calculated between each specimen and the Procrustes average for the sample (Gunz & Mitteroecker, 2013). This sliding process renders these landmarks geometrically homologous, at which point they are converted into shape coordinates using generalised least squares Procrustes superimposition

(Gower, 1975; Rohlf & Slice, 1990).

6. Geometric morphometric analysis and visualisation of shape variation

A principal components analysis (PCA) was conducted using the

Fig. 6. Plot of the first and second principal components of an analysis of the isolated lingual ridge shape variation between molars with variable expression of a LAC. (B) Centroid size of macaque lower second molars with and without a LAC. (C) Exaggerated wireframe model of the shape change along PC1 (exaggerations defined as two standard deviations from the mean.) Lingual view. (D) Exaggerated wireframe model of the shape change along PC2. Lingual view.
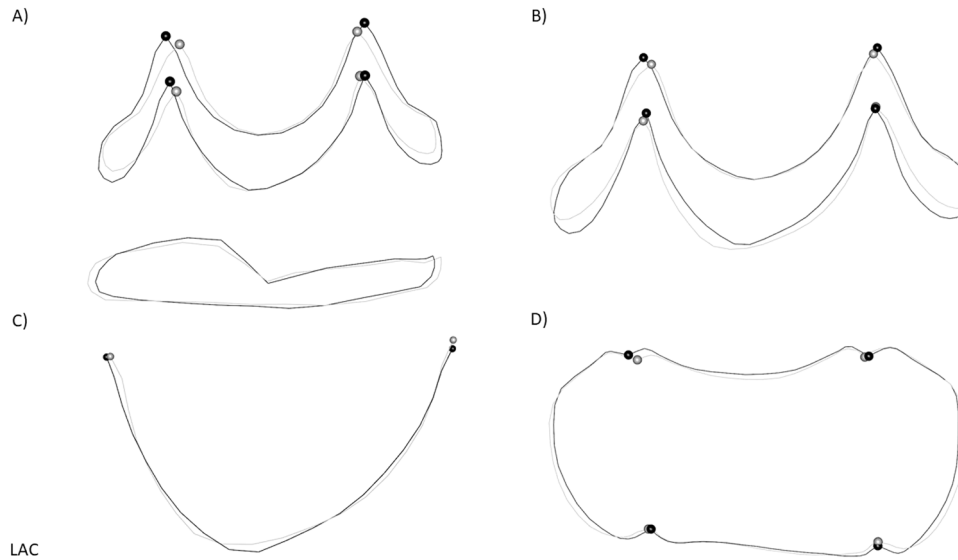
Fig. 7. Mean landmark configurations for specimens with and without a LAC. Black = LAC absent. Grey = LAC present. (A) Whole tooth mean model. Lingual view; (B) EDJ ridge mean model. Lingual view; (C) Isolated lingual ridge mean model. Lingual view; (D) EDJ ridge mean model. Occlusal view.

Procrustes coordinates of each specimen in shape space. This was conducted on three different sets of EDJ landmarks for both the LAC and DAC: a complete analysis including the EDJ and CEJ landmarks, a marginal ridge analysis that excluded the CEJ and only consisted of EDJ_MAIN and EDJ_RIDGE landmarks, and an isolated ridge analysis that only included the ridge landmarks between the two dentine horns where the accessory cusp is found (isolated distal ridge between the hypoconid and entoconid for the DAC analysis, and isolated lingual ridge between the metaconid and entoconid for the LAC analysis). 2D and 3D PCA plots (whole tooth, marginal ridge, and isolated ridge) were generated to summarize variation in EDJ shape between the 'Present' and 'Absent' groups. Wireframe models were then used to visualise the shape changes along the first two PCs. Shape changes in the wireframes provided have been exaggerated to display the shape of a hypothetical specimen occupying the extreme ends of each PC, and are depicted as two standard deviations from the mean. The size of specimens was analysed using the natural logarithm of centroid size and visualised through boxplots.

Fig. 8. 3D plot of the first three principal components of an analysis of EDJ ridge shape variation between specimens with variable expression of a DAC. Accessory cusp absence corresponds to the lighter grey convex hull and grey spheres. Accessory cusp presence corresponds to the darker grey convex hull and black spheres. 3D plots of the whole tooth analysis and isolated distal ridge are provided in the supplementary materials.
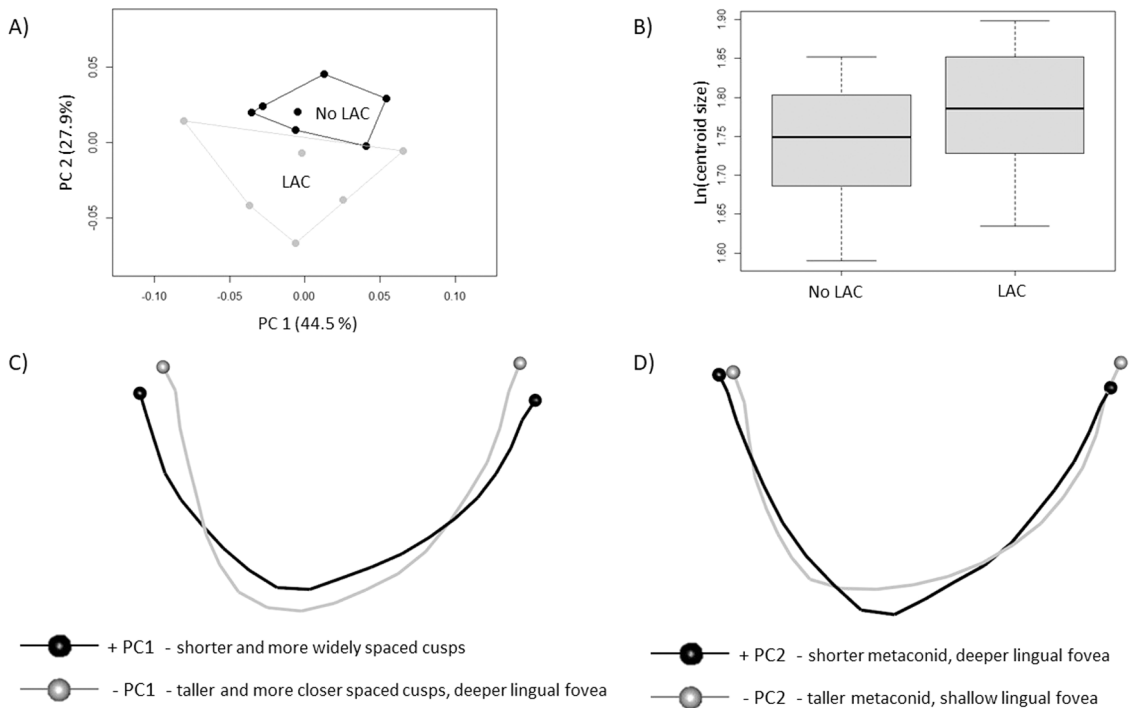
Fig. 9. (A) Plot of the first and second principal components of an analysis of whole tooth shape variation between molars with variable expression of a DAC. (B) Centroid size of macaque lower second molars with and without a DAC. (C) Exaggerated wireframe model of the shape change along PC1 (exaggerations defined as two standard deviations from the mean). Lingual view. (D) Exaggerated wireframe model of the shape change along PC2. Lingual view.

7. Results

7.1. Lingual accessory cusp analysis

Principal component analysis of EDJ and CEJ shape reveals that molars with lingual accessory cusps are distinct from those without an accessory cusp. The 3D PCA plots show clear separation of the 'Present' and 'Absent' categories in all three analyses (Fig. 3 and Supplementary Figures 2 and 3). A 2D PCA of the whole tooth shows overlap along PC1 and PC2, but with a tendency towards the presence of a LAC along the
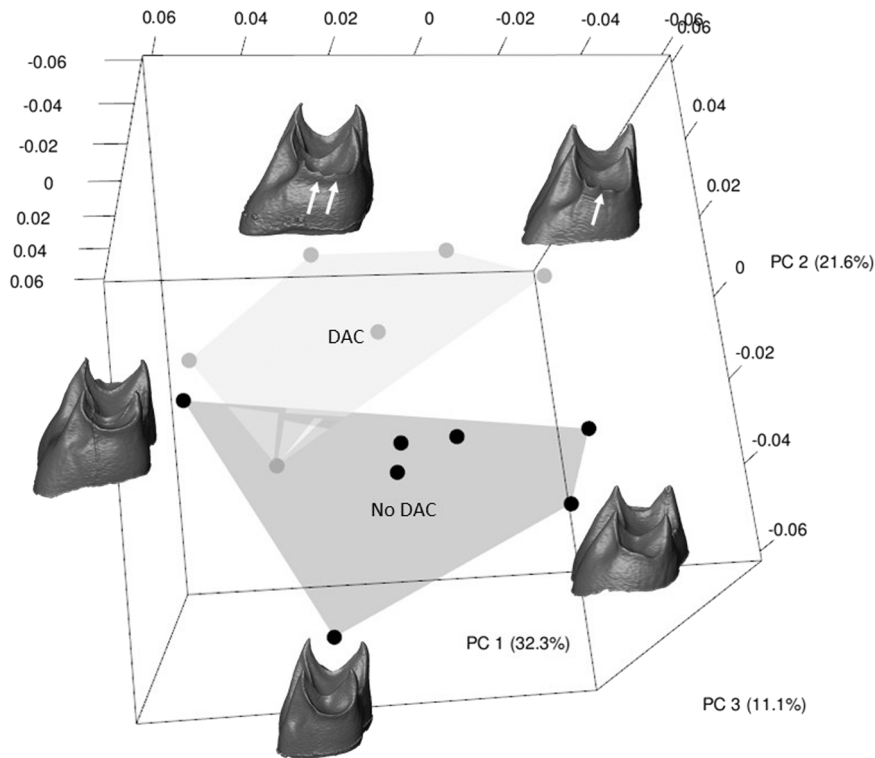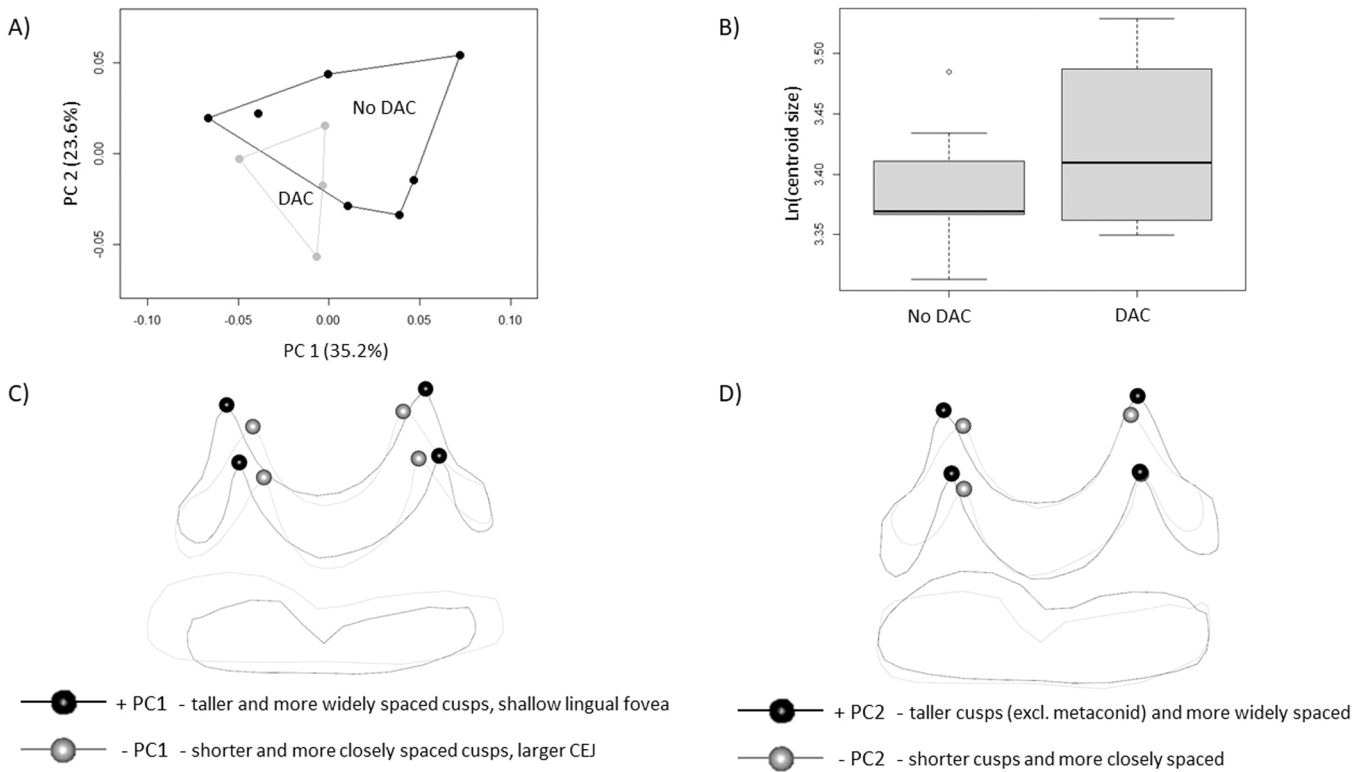

Fig. 10. Plot of the first and second principal components of an analysis of EDJ ridge shape variation between molars with variable expression of a DAC. (B) Centroid size of macaque lower second molars with and without a DAC. (C) Exaggerated wireframe model of the shape change along PC1 (exaggerations defined as two standard deviations from the mean.) Lingual view. (D) Exaggerated wireframe model of the shape change along PC2. Lingual view.
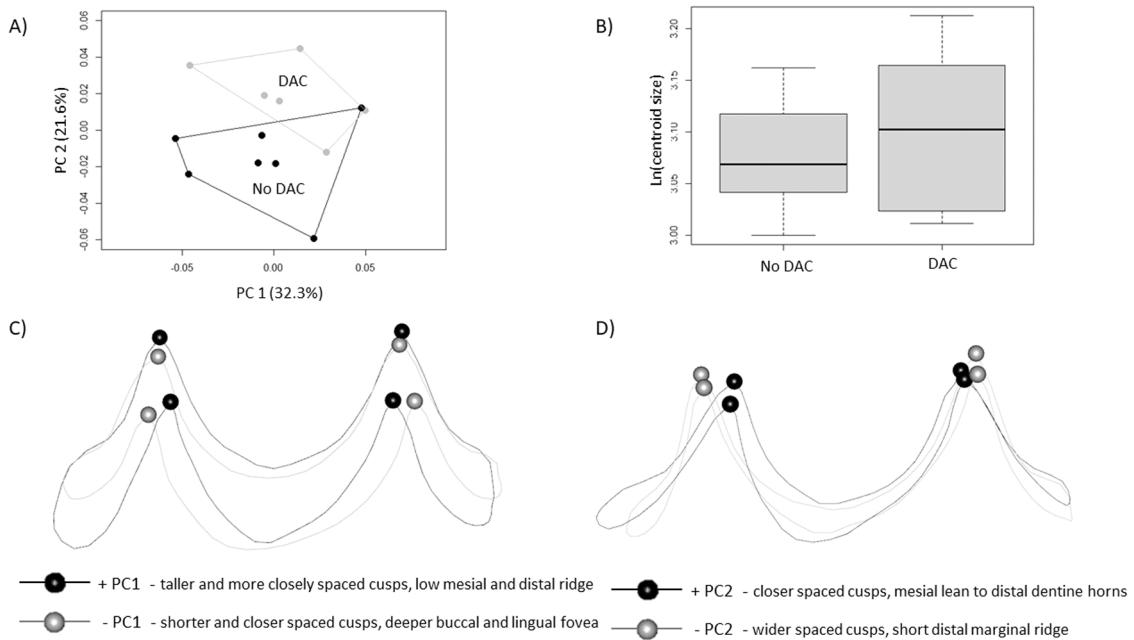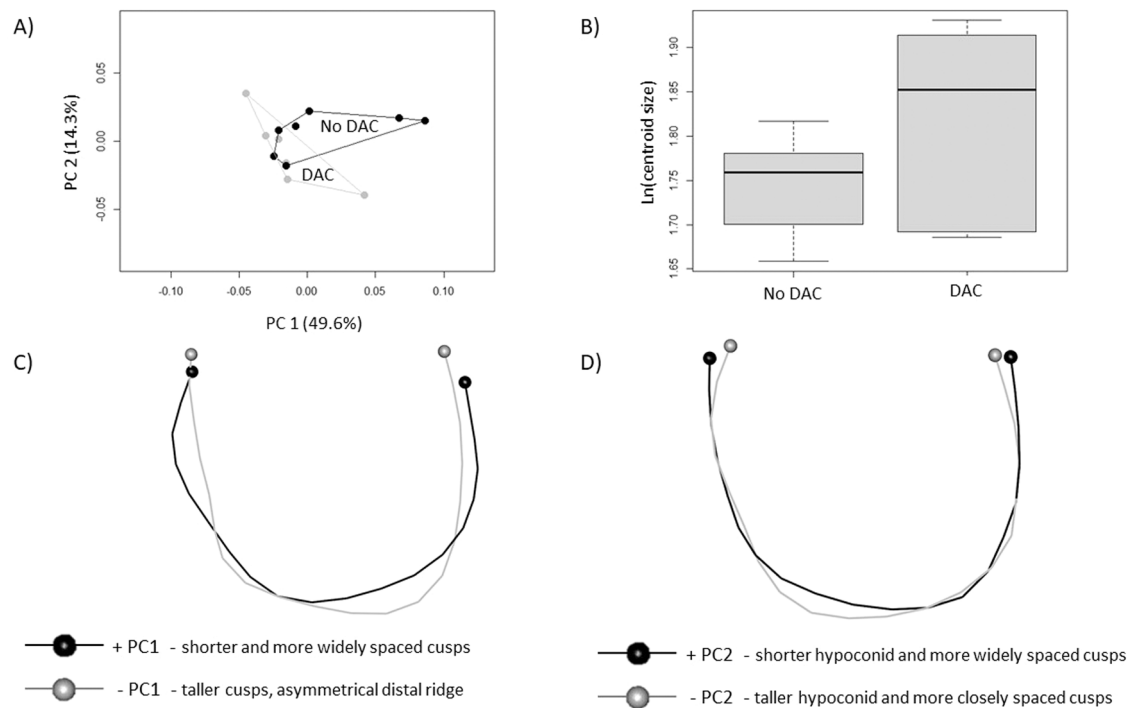
Fig. 11. Plot of the first and second principal components of an analysis of the isolated distal ridge shape variation between molars with variable expression of a DAC. (B) Centroid size of macaque lower second molars with and without a DAC. (C) Exaggerated wireframe model of the shape change along PC1 (exaggerations defined as two standard deviations from the mean.) Distal view. (D) Exaggerated wireframe model of the shape change along PC2. Distal view.

negative end of each PC (Fig. 4). The corresponding wireframes reveal that the negative end of both PC1 and PC2 are characterized by smaller and more closely spaced mesial and distal cusps, and a deeper marginal ridge gradient.

Boxplots of centroid size for the whole tooth analysis show that molars with LACs tend to be slightly larger than those without (Fig. 4), although this was a non-significant trend (p = 0.162). A 2D PCA of just the marginal ridge shows clear separation between groups within the first and second principal components (Fig. 5), with a tendency towards the presence of a LAC along the negative end of PC1 (slightly smaller and widely-spaced cusps and a wider and deeper lingual fovea) and positive end of PC 2 (slightly shorter and more closely-spaced cusps, and a deeper and more asymmetrical lingual fovea). For the isolated lingual ridge, the groups overlap completely along PC1, but separate well along PC2 (Fig. 6). Accessory cusp presence is found along the negative end of PC2, which is associated with a lingual ridge with a slightly taller metaconid, and a shallow and asymmetrical marginal ridge. Boxplots of centroid size for the EDJ ridge and isolated ridge show a similar trend of LAC presence among larger molars, but with a greater overlap between the groups and a statistically non-significant trend (p = 0.628 and p = 0.436 respectively).

We also examined the mean landmark configurations in each analysis for those specimens with and without a LAC (Fig. 7). In the whole tooth landmark set, specimens with a LAC exhibited slightly shorter entoconid and buccal dentine horns, and closer spaced mesial and distal cusps. For the marginal ridge analysis, specimens with a LAC again exhibited slightly reduced entoconid height, but also a deeper lingual fovea. These findings match the results seen in the exaggerated wireframes, but highlight the subtly of these differences between the groups. For the lingual ridge landmark set, those with and those without a LAC display a slight difference in metaconid height, with negligible other differences. Mean landmark configurations of the occlusal view of the marginal ridge also reveal negligible differences between the groups from this angle.

8. Distal accessory cusp analysis

Principal component analysis EDJ shape reveal that molars with distal accessory cusps are morphologically distinct from those without an accessory cusp. The 3D PCA plots show clear separation of the 'Present' and 'Absent' categories in the whole tooth and isolated ridge analysis (Supplementary Figures 4 and 5). For the EDJ ridge analysis, a 3D PCA shows one individual with an accessory cusp within the convex hull of the 'Absent' grouping (Fig. 8). A 2D PCA of the whole tooth shows no separation of the groups along PC1 or PC2 (Fig. 9). A 2D PCA of just the marginal ridge shows no separation along PC1, but a tendency towards DAC presence along the positive end of PC2 (Fig. 10). Wireframes reveal that the positive end of PC2 is exemplified by more closely spaced mesial and distal cusps, and a distally extended marginal ridge that creates a less acute gradient of the rising distal ridge. A 2D PCA of the isolated distal ridge shows no separation of the groups along PC1 or PC2 (Fig. 11). Boxplots of centroid size for all analyses show that molars with DAC are slightly larger than those without, but were all statistically non-significant results (whole tooth p = 0.471, EDJ ridge p = 0.549, distal ridge p = 0.151).

Examination of the mean landmark configurations in each DAC analysis reveals a consistent trend towards closer spaced mesial and distal dentine horns among those with an accessory cusp. In the whole tooth landmark set, this is combined with a slightly wider distal extension of the CEJ ridge. In the marginal ridge landmark set, closer spaced mesial and distal primary dentine horns among those with a DAC are also associated with the less acute gradient of the rising distal ridge and extended marginal ridge seen in the exaggerated wireframes. For the distal ridge landmark set, specimens with a DAC exhibited slightly closer spaced and taller distal cusps in a lingual view, however these differences were subtle. The occlusal view of the marginal ridge provides an alternative angle with which to observe the extended distal ridge in specimens with a DAC.

9. Discussion

Principal component analysis of EDJ and CEJ shape demonstrates that macaque molars with accessory cusps are morphologically distinct from those without accessory cusps. In five of the six analyses, 3D PCA plots showed complete separation (with only a slight overlap of the convex hulls in the EDJ ridge analysis of the DAC). To understand these shape differences and determine whether they matched the predictions of the patterning cascade model of cusp development, shape changes along the first two PCs and between the average shape of molars with and without accessory cusps were assessed from wireframes. When examining the shape of the whole tooth, LAC presence was associated with smaller and more closely spaced primary cusps. While smaller cusps among the 'Present' category match the predictions of the patterning cascade model, more closely spaced cusps are thought to reduce the available space for cusp initiation and inhibit the formation of additional cusps. In the EDJ ridge analysis, LAC presence was again associated with shorter primary cusps along both PCs in the exaggerated wireframes. The mean landmark configurations confirm this tendency toward reduced entoconid height among specimens with LAC, while demonstrating negligible differences in cusp spacing. Although there is no clear trend regarding cusp spacing in these results, LAC presence was consistently associated with shorter primary cusps in these analyses (particularly regarding the height of the entoconid), which is compatible with the predictions of the patterning cascade model.

For the DAC analyses, both the mean landmark configurations and exaggerated wireframes demonstrate an important trend in cusp positioning that may be responsible for differences in distal marginal ridge morphology and subsequent accessory cusp formation. While DAC presence was associated with slightly shorter primary cusps in some analyses, it was consistently associated with significantly more mesially positioned distal dentine horns. The mesial positioning of the distal cusps may be responsible for the increased extension of the distal marginal ridge seen in both the mean models and wireframes, providing more potential space for accessory cusp formation. Ortiz et al. (2018) has previously shown in hominoid molars that small intercusp differences correlate with the presence of cusps on the peripheral region of the crown. While distal accessory cusps in macaque molars might not meet the criteria of a peripheral cusp, in that they still form on the marginal ridge of the tooth, these results do suggest that the positioning of the primary cusps contribute to the formation of accessory cusps, particularly if more closely-spaced cusps allow for increased peripheral space on the crown surface.

For the isolated ridge analyses, LAC presence was associated with a slightly taller metaconid, but also a more shallow and asymmetrical lingual ridge. Currently, the processes responsible for crest formation in mammalian dentitions are poorly understood. Li et al. (2018) have shown how dental crests in muroid molars are linked to FGF expression. For example, in gerbil molars, a linear expression pattern of Fgf4 facilitates the formation of long, flat crests (or lophs) instead of cusps. Modifying this Fgf signalling in gerbil tooth germs transforms the shape of the epithelium and converts crests into cusps. As FGFs are the established candidates for EK inhibition (Salazar-Ciudad & Jernvall, 2002), it is unknown whether crest development between primary enamel knots could influence or interfere with enamel knot initiation at the location of later forming cusps. Furthermore, it is also worth considering whether later processes of enamel and dentine mineralisation could alter the shape of the EDJ and create morphological complexity that was not present during the active period of the enamel knots.

For the isolated distal ridge, the mean models demonstrate minimal differences in ridge morphology between the groups, but show that DAC presence was associated with slightly taller and closer spaced distal cusps. While this does not match the predictions of the patterning cascade model, based on the potential importance of the mesial positioning of the distal cusps relative to the tooth germ, it may be that

slightly taller distal cusps have an insignificant effect on potential accessory cusp formation in these peripheral regions of the tooth.

Boxplots of centroid size for all the analyses demonstrate that molars with accessory cusps tend to be larger than those without accessory cusps, although differences were statistically non-significant in this small sample. While not reaching statistical significance, this consistent trend matches the predictions of the patterning cascade model, as larger teeth have more space for additional cusp formation (Salazar-Ciudad & Jernvall, 2002, 2010).

While the patterning cascade model appears to be useful in providing some explanation for the variable presence of accessory cusps in primate dentitions, there are aspects of macaque molar morphology that indicate the existence of other developmental processes in the formation of additional cusps. While accessory cusp scoring was restricted only to 'Absent' and 'Present' categories to maximise the sample size of each group, the occurrence of multiple, closely positioned accessory cusps along a single marginal ridge in this sample raises interesting questions regarding the processes and epigenetic conditions that could lead to such a phenomenon. In the dental literature, these features have previously been described as 'double' or 'split' cusps (Wood & Abbott, 1983; Aiello & Dean, 1990; Keene, 1994). Based on observations of accessory cusp patterning at the EDJ surface, Skinner and Gunz (2010) have suggested that these terms may misrepresent the true developmental processes underlying the formation of these features. To date, Martin et al. (2017) has provided the most convincing observations of what might be considered true twinned or split dentine horns in fossil hominins, demonstrating the presence of multiple dentine horns of similar size and shape near the apex of a primary cusp tip. Importantly, these features appear morphologically distinct from the more commonly observed manifestations of multiple dentine horns present in this sample (Fig. 1) and among many other primate taxa.

In rare cases, the expression of multiple dentine horns between primary cusps appears to directly reflect the iterative process one would expect from a patterning cascade model, with progressively smaller cusps forming along a ridge as development progresses towards the CEJ (see Skinner & Gunz, 2010, Fig. 3 D). In the majority of cases however, multiple accessory cusps instead appear as closely spaced and equally sized dentine horns. Currently, it is difficult to conceptualize how these features could occur under the patterning cascade model when the enamel knot of one dentine horn should inhibit the development of the other. Histological studies of mouse molars have noted the presence of a novel epithelial cell cluster after the disappearance of the SEK, which has been named the tertiary enamel knot (Luukko et al., 2003). If tertiary enamel knots are also present in other mammalian taxa, is conceivable that they may be responsible for accessory cusp expression here. As tertiary enamel knots appear to express some, but not all, of the signalling molecules present in secondary enamel knots (Luukko et al., 2003), there may be different constraints imposed by the tertiary enamel knots that leads to the occurrence of this variation (Jernvall, 2000). Ultimately, while the patterning cascade model seems to be useful for interpreting variation in single-cusp expression, additional research is required to understand the phenomenon of closely spaced accessory cusp patterns on the same region of the marginal ridge in primates. This research may also benefit from considering other competing or complimentary models, such as the model of growth restraint by Osborn (2008), which acknowledges the physical and mechanical constraints on the developing enamel organ during proliferation and how directional forces within the tooth germ may contribute to buckling of the epithelium and final crown shape.

Chapple and Skinner (2023a) have recently discussed the typical patterns of cusp expression in primate molars, highlighting numerous locations on the EDJ surface where accessory cusp are very rarely seen. In the current study we note that, while lingual and distal accessory cusps were commonly observed in the macaque sample, no cusps were observed on the buccal or mesial marginal ridges. As primary cusp size and spacing is relatively symmetrical between buccal and lingual, and
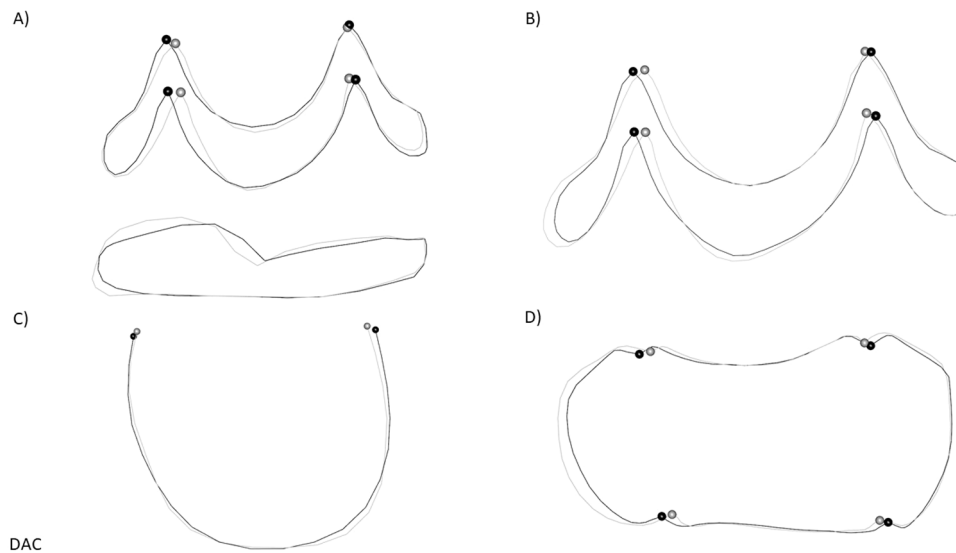
Fig. 12. Mean landmark configurations for specimens with and without a DAC. Black = DAC absent. Grey = DAC present. (A) Whole tooth mean model. Lingual view.; (B) EDJ ridge mean model. Lingual view; (C) Isolated distal ridge mean model. Distal view; (D) EDJ ridge mean model. Occlusal view.

mesial and distal sides of the tooth crown, we should expect to see the variable expression of cusps on all marginal ridge locations if the patterning cascade model was the only mechanism regulating enamel knot initiation. Furthermore, in no cases was an accessory cusp observed within the occlusal basin of the tooth. As noted in Chapple and Skinner (2023b) this is consistent with a development constraint in cusp patterning in that enamel knots initiation appears to be linked to crests. Overall, our results indicate that parameters of the patterning cascade model are components of the variation in cusp expression in primate molar morphology, but are they not the only source of developmental constraint.

This study underscores the importance of recognising the developmental processes responsible for tooth crown morphology in primates. Cusp patterning plays an important role in studies of primate systematics and taxonomy, and relies heavily on the assumption that these features are of phylogenetic relevance. This study contributes to an emerging picture that cusp patterning may be determined by subtle changes in the developmental parameters of the patterning cascade model, which themselves may be established during the early stages of development of the tooth germ. Instead of attributing the relatively predictable presence of a particular accessory cusp in a certain primate clade or human population to the inheritance or conservation of a specific genetic programme, it may be more appropriate to consider it a reflection of differences in cusp positioning and/or tooth size, which themselves carry some genetic component. While we suspect the patterning cascade model to be only one source of constraint in primate cusp formation, the acknowledgement of these developmental mechanisms is crucial for the proper interpretation of tooth crown morphology in primate taxonomy and systematics..

CRediT authorship contribution statement

Simon Andrew Chapple: Writing – review & editing, Writing – original draft, Methodology, Formal analysis, Conceptualization. **Matthew M. Skinner:** Writing – review & editing, Supervision, Methodology, Investigation, Data curation, Conceptualization. **Tanya M. Smith:** Writing – review & editing, Validation, Data curation.

Declaration of Competing Interest

The authors have no competing interest to disclose.

Appendix A. Supporting information

Supplementary data associated with this article can be found in the online version at doi:10.1016/j.archoralbio.2024.106067.

References

Aiello, L., Dean, C. (1990). *An Introduction to Human Evolutionary Anatomy.* Academic Press.

Cannoodt, R., Bengtsson, H. (2019). rcannood/princurve: princurve (Version 2.1.4) [computer software]. Zenodo https://doi.org/10.5281/zenodo.3351282.

Chapple, S. A., & Skinner, M. M. (2023a). Primate tooth crown nomenclature revisited. *PeerJ, 11,* Article e14523.

Chapple, S. A., & Skinner, M. M. (2023b). A tooth crown morphology framework for interpreting the diversity of primate dentitions. *Evolutionary Anthropology, 32*(5), 240–255.

Davies, T. W., Alemseged, Z., Gidna, A., Hublin, J. J., Kimbel, W. H., Kullmer, O., Spoor, F., Zanolli, C., & Skinner, M. M. (2021). Accessory cusp expression at the enamel-dentine junction of hominin mandibular molars. *PeerJ, 9,* Article e11415.

Feeney, R. N., Zermeno, J. P., Reid, D. J., Nakashima, S., Sano, H., Bahar, A., Hublin, J. J., & Smith, T. M. (2010). Enamel thickness in Asian human canines and premolars. *Anthropological Science, 118,* 191–198.

Gower, J. C. (1975). Generalized procrustes analysis. *Psychometrika, 40,* 33–51.

Gunz, P., & Mitteroecker, P. (2013). Semilandmarks: a method for quantifying curves and surfaces. *Hystrix, the Italian Journal of Mammalogy, 24*(1), 103–109.

Gunz, P., Mitteroecker, P., & Bookstein, F. L. (2005). Semilandmarks in three dimensions. *In Modern Morphometrics in Physical Anthropology,* 73–98 (Springer, Boston, MA).

Harris, E. F. (2007). Carabelli's trait and tooth size of human maxillary first molars. *American Journal of Physical Anthropology, 132*(2), 238–246.

Jernvall, J. (2000). Linking development with generation of novelty in mammalian teeth. *Proceedings of the National Academy of Sciences, 97,* 2641–2645.

Jernvall, J., & Thesleff, I. (2000). Reiterative signaling and patterning during mammalian tooth morphogenesis. *Mechanisms of Development, 92*, 19–29.

Kassai, Y., Munne, P., Hotta, Y., Penttilä, E., Kavanagh, K., Ohbayashi, N., Takada, S., Thesleff, I., Jernvall, J., & Itoh, N. (2005). Regulation of mammalian tooth cusp patterning by ectodin. *Science, 309*, 2067–2070.

Kato, A., Tang, N., Borries, C., Papakyrikos, A. M., Hinde, K., Miller, E., Kunimatsu, Y., Hirasaki, E., Shimizu, D., & Smith, T. M. (2014). Intra-and interspecific variation in macaque molar enamel thickness. *American Journal of Physical Anthropology, 155*, 447–459.

Keene, H. J. (1994). On the classification of C6 (tuberculum sextum) of the mandibular molars. *Human Evolution, 9*, 231–247.

Kondo, S., & Townsend, G. C. (2006). Associations between Carabelli trait and cusp areas in human permanent maxillary first molars. *American Journal of Physical Anthropology, 129*, 196–203.

Li, L., Tang, Q., Kwon, H. J., Wu, Z., Kim, E. J., & Jung, H. S. (2018). An explanation for how FGFs predict species-specific tooth cusp patterns. *Journal of Dental Research, 97*(7), 828–834.

Luukko, K., Løes, S., Furmanek, T., Fjeld, K., Kvinnsland, I. H., & Kettunen, P. (2003). Identification of a novel putative signaling center, the tertiary enamel knot in the postnatal mouse molar tooth. *Mechanisms of Development, 120*(3), 270–276.

Martin, R. M., Hublin, J. J., Gunz, P., & Skinner, M. M. (2017). The morphology of the enamel–dentine junction in Neanderthal molars: Gross morphology, non-metric traits, and temporal trends. *Journal of Human Evolution, 103*, 20–44.

Monson, T.A. (2012). *Metameric Variation in the Expression of the Interconulus in Papio and Macaca* (Doctoral dissertation, San Francisco State University).

Niswander, L., & Martin, G. R. (1992). Fgf-4 expression during gastrulation, myogenesis, limb and tooth development in the mouse. *Development, 114*, 755–768.

Olejniczak, A. J., Tafforeau, P., Smith, T. M., Temming, H., & Hublin, J. J. (2007). Compatibility of microtomographic imaging systems for dental measurements. *American Journal of Physical Anthropology, 134*, 130–134.

Ortiz, A., Bailey, S. E., Schwartz, G. T., Hublin, J. J., & Skinner, M. M. (2018). Evo-devo models of tooth development and the origin of hominoid molar diversity. *Science Advances, 4*, Article eaar2334.

Osborn, J. W. (2008). A model of growth restraints to explain the development and evolution of tooth shapes in mammals. *Journal of Theoretical Biology, 255*(3), 338–343.

Rohlf, F. J., & Slice, D. (1990). Extensions of the Procrustes method for the optimal superimposition of landmarks. *Systematic Zoology, 39*(1), 40–59.

Salazar-Ciudad, I., & Jernvall, J. (2002). A gene network model accounting for development and evolution of mammalian teeth. *Proceedings of the National Academy of Sciences of the United States of America, 99*, 8116.

Salazar-Ciudad, I., & Jernvall, J. (2010). A computational model of teeth and the developmental origins of morphological variation. *Nature, 464*, 583–586.

Schulze, M. A., & Pearce, J. A. (1994). A morphology-based filter structure for edge-enhancing smoothing. *In Proceedings of 1st International Conference on Image Processing,* (pp. 530–534). IEEE,.

Schlager, S., Zheng, G., Li, S., and Szekely, G. (2017). Statistical Shape and Deformation Analysis. In *Morpho and Rvcg–Shape Analysis in R: R-packages for geometric morphometrics, shape analysis and surface manipulations. (pp. 217–56). Academic press.*

Skinner, M. M., & Gunz, P. (2010). The presence of accessory cusps in chimpanzee lower molars is consistent with a patterning cascade model of development. *Journal of Anatomy, 217*, 245–253.

Skinner, M. M., Wood, B. A., Boesch, C., Olejniczak, A. J., Rosas, A., Smith, T. M., & Hublin, J. J. (2008). Dental trait expression at the enamel-dentine junction of lower molars in extant and fossil hominoids. *Journal of Human Evolution, 54*, 173–186.

Smith, T. M., Olejniczak, A. J., Zermeno, J. P., Tafforeau, P., Skinner, M. M., Hoffmann, A., Radovčić, J., Toussaint, M., Kruszynski, R., Menter, C., & Moggi-Cecchi, J. (2012). Variation in enamel thickness within the genus Homo. *Journal of Human Evolution, 62*, 395–411.

Swindler, D. R. (1983). Variation and homology of the primate hypoconulid. *Folia Primatologica, 41*(1-2), 112–123.

Swindler, D. R. (2002). *Primate dentition: an introduction to the teeth of non-human primates (Vol. 32).* Cambridge University Press.

Szalay, F. S., & Delson, E. (2013). *Evolutionary history of the primates.* Academic Press.

Thesleff, I., & Nieminen, P. (1996). Tooth morphogenesis and cell differentiation. *Current Opinion in Cell Biology, 8*, 844–850.

Vaahtokari, A., Åberg, T., Jernvall, J., Keränen, S., & Thesleff, I. (1996). The enamel knot as a signaling center in the developing mouse tooth. *Mechanisms of Development, 54*, 39–43.

Winchester, J.M. (2016). *Molar topographic shape as a system for inferring functional morphology and developmental patterning in extant cercopithecoids* (Doctoral dissertation, The Graduate School, Stony Brook University: Stony Brook, NY).

Wood, B. A., & Abbott, S. A. (1983). Analysis of the dental morphology of Plio-pleistocene hominids. I. Mandibular molars: Crown area measurements and morphological traits. *Journal of Anatomy, 136*, 197.

Wollny, G., Kellman, P., Ledesma-Carbayo, M. J., Skinner, M. M., Hublin, J. J., & Hierl, T. (2013). MIA-A free and open source software for gray scale medical image analysis. *Source Code for Biology and Medicine, 8*(1), 20.